

Numerical analysis of the structural response of masonry columns confined with SRG (Steel Reinforced Grout)

Luciano Ombres¹, Salvatore Verre²

¹*Department of Civil Engineering, University of Calabria, Arcavacata di Rende (CS) Italy luciano.ombres@unical.it, (corresponding author);*

²*Department of Civil Engineering, University of Calabria, Arcavacata di Rende (CS) Italy salvatore.verre@unical.it.*

Abstract – In recent decades the composite materials have been used to strengthened and repair the historical masonry. A new class of composites that is begin explored that includes steel fiber sheet embedded in an inorganic matrix. The use of steel fibers was proposed in alternative to others fibers as PBO, Carbon glass and Basalt. In the paper, the structural behavior of masonry columns strengthened with steel-FRCM (SRG) have been investigated through the numerical 3D simulations calibrated on experimental tests present in literature. The 3D numerical approach is based on a macro-model to simulate the nonlinear structural behavior masonry columns. The comparison of the numerical models with the experimental carryout shows in terms of peak force and axial force–strain curves.

I. INTRODUCTION

Fiber reinforced composite, especially fiber reinforced polymer (FRP) composites, buy jacketing of columns is a very widespread technique in a large number of rehabilitation in the seismic events.

Several advantages are related to the use of FRPs to strengthen existing structures; among these the high strength to weight ratio, corrosion resistance, ease and speed of application, and minimal change of geometry. Despite all these advantages, the FRP retrofitting technique has a few drawbacks mainly attributed to the organic epoxy resins used to bind the fibers; poor fire resistance; high costs; inapplicability on wet surfaces or at low temperatures; hazards for the manual worker; diffusion tightness, poor thermal compatibility with the base material; susceptibility to UV radiation and low reversibility. FRCM composites are known under different acronyms in the literature such as textile reinforced concrete (TRC) [1-2], textile reinforced mortar (TRM) [3-4], and mineral based composites (MBC) [5]. Typically, FRCM composites consist of fabric meshes with fibers arranged in two orthogonal directions and bonded to the substrate with a cement-based mortar. The

type of matrix employed in FRCM composites [6-8] is generally characterized by: 1) high resistance to fire and high temperature; 2) resistance to UV radiation; 3) ease of handling during application because the inorganic binder is water- based; 4) permeability compatibility with the concrete substrate; and 5) unvarying workability time (between 4 °C and 40 °C). A new class of composites that is being explored includes steel fiber sheets with either an inorganic matrix or an organic matrix described above. The use of steel fibers was proposed as a lower- cost alternative to other fiber types used in FRCM or FRP previously described. Scientific works on Steel Reinforced Grout (SRG) systems [9] showed the potentialities of these innovative composite materials in improving structural performance on the concrete members. A very few studies have been reported on the bond behavior of SRG-masonry joints. The numerical analysis of this problem is also quite complex but, at least, the usually fundamental aspect of the bond between SRG and the substrate can be considered here as less critical since the closed shape of the reinforcement suggests that the material failure should be the driving phenomenon. Following this approach, in the numerical models there is perfect bond between matrix and the steel fibers.

In this preliminary study the focus was to study a numerical simulation considered the macro model approach, without the distinction between mortar and brick of the masonry. Finally, this model was compared with the experimental study present in literature [10] in terms of the peak load and the axial force-strain curves.

II. MATERIAL CONSTITUTIVE LAW AND SOLUTION TECHNIQUE

To verify the role of the reinforcement wrapped around the columns, some numerical modeling has been developed. The numerical analysis, conducted by Abaqus [11], is performed using concrete damage plasticity (CDP) material model. The CDP model is based on the

assumption of a scalar isotropic damage with different damage description in tension and in compression. Moreover, it is particularly suitable for applications in which the material exhibits damage, especially under loading–unloading conditions, or in the case of dynamic analyses. In CDP two main failure mechanisms can be defined: the tensile cracking and the compressive crushing to define the elastic and plastic range. The linear range of the behavior was defined by density ($\rho=1.70 \text{ g/cm}^3$), the elastic modulus (E_m) and the Poisson's ratio (ν). While, in the plastic range the damage parameters should be defined for the tensile/compressive behavior. In addition, the plastic range was characterized by the following five parameters: dilation angle (38°), the potential eccentricity (0.1), the ratio of initial biaxial compressive yield stress to initial uniaxial compressive yield stress (1.16), the ratio of the second stress invariant on the tensile meridian to that on the compressive meridian (0.667) and the viscosity parameter (0.0).

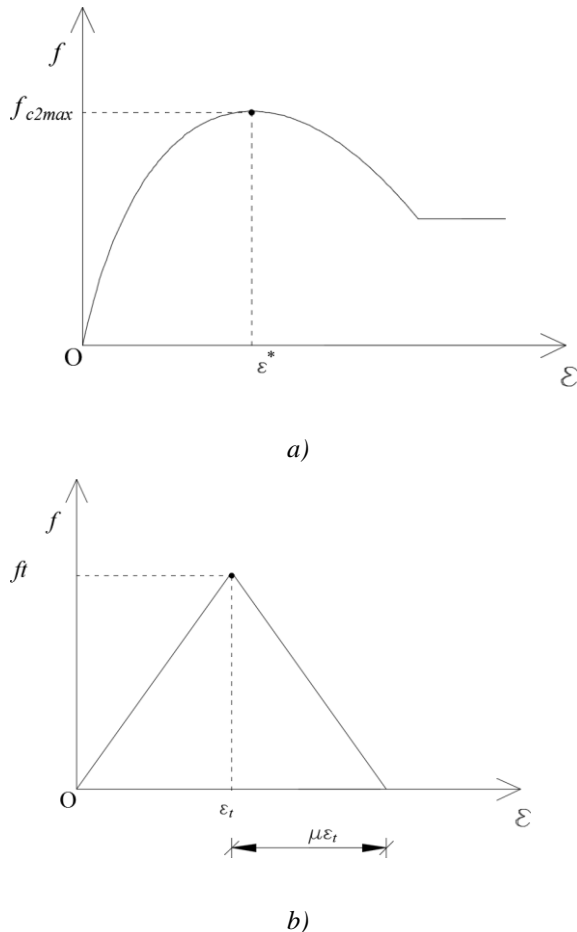


Fig. 1. Constitutive laws: a) Compression, and b) Tension.

The constitutive law is able to take into account the

increase of the strength according to Vecchio and Collins [12], while the tensile stress was modeled with linear elastic branch until of the peak strength, f_t , and a subsequent non-linear descending branch describing the tension stiffening effect. As values f_{c2max} for both the columns strengthening and the un-strengthening were considered the average of the peak axial stress presented in [10]

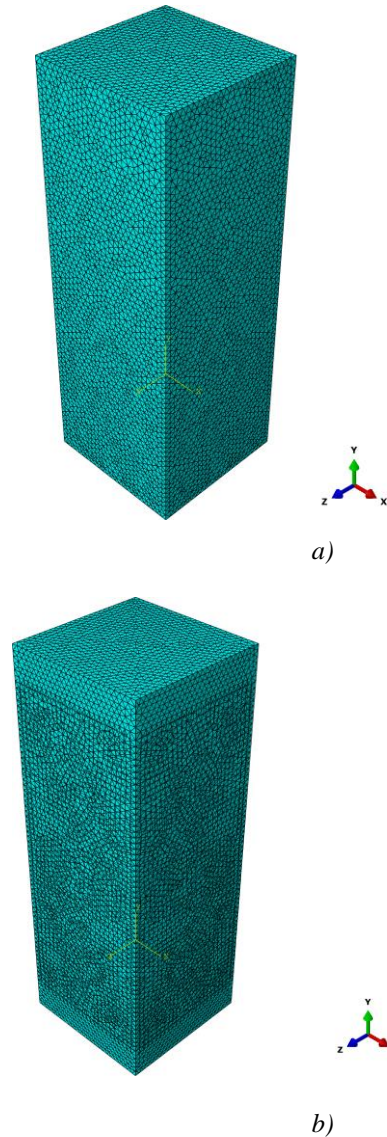


Fig. 2. FE Mesh: a) un-strengthened, and b) strengthened masonry columns

The external reinforcement was modeled by S4 shell with linear interpolation functions. The nonlinear analysis was conducted by adopting a resolution by dynamic approach. To obtain a static type solution, the kinetic

energy should be compared with the internal energy of the model during the analysis, so that, the value does not exceed 5%, and the variable mass scaling was used at the beginning of each step at a fixed time increment equal to 0.00005 in all the regions of the model [13]. The analysis was carried out by control displacement in order to simulate the softening branch of the load displacement deflection curve and the deboning process. All the tests unwrapped and strengthened columns considered were modeled in three-dimension (3D). In additions, the specimens were clumped at base. In this preliminary work was considered the macro model approach, without the distinction between mortar and brick of the masonry, using the single equivalent material characterized of the unique constitutive law. The model was modeled by using C3D4, which is based on a tetrahedral geometry with linear interpolation functions.

The strengthened system considered is the SRG system was modeled as a homogenous elastic material until failure; the input parameters were defined by density ($\rho=7.85 \text{ g/cm}^3$), the elastic modulus (E_f) in according to the manufacture's recommendation, and Poisson's ratio ($\nu=0.2$). Typical failure is interlaminar failure (delamination) of the matrix has also been reported for other types of SRG composites in previous studies [9-10-14], in addition to slippage of the fibers from the embedding matrix, detachment of the composite strip at the SRG-matrix interface, or fiber fracture. In this preliminary study, the perfect bond was considered as interaction between the masonry column and the external reinforcement.

III. EXPERIMENTAL INVESTIGATION

To evaluate the effectiveness to the SRG system were considered two experimental campaigns present in literature [10-14].

In both experiments the masonry columns considered of solid clay brick units with nominal dimension of 120 mm (width) x 55 mm (height) x 250 mm (length) and a relatively low strength mortar. The thickness of the mortar joints was 10 mm.

Table 1. Physical and mechanical properties of the steel fibers [15].

Fabric density	670 g/m ²
Wire characteristic tensile stress	>2900MPa
Wire elastic modulus	>205GPa
Sheet break deformation	>2%
Number of cord/cm	1.57 cords/cm
Mass	≈670 g/m ²

For the confined specimens, the steel fibers embedded in an inorganic mortar matrix. Three of the five filaments are straight, and the remaining two filaments are wrapped around the other three with a high torque angle and the cross-sectional area of the cord is 0.538 mm².

The physical and mechanical properties of the matrix provided by the manufacture [15] are reported in Table 1.

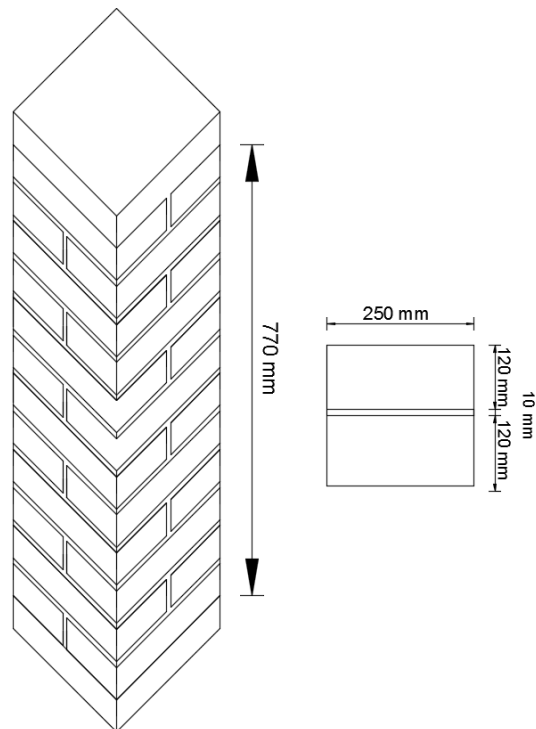


Fig. 3. Geometrical dimension of the specimens.

IV. NUMERICAL/EXPERIMENTAL COMPARISON

The comparison between the experimental results [10] and those of the numerical model for unstrengthening and strengthened columns described in the precedent section were reported in the following.

Table 2 reports the axial strength values for both confined and unconfined masonry columns measured by tests [10] and predicted by the numerical model. The analysis of results evidences that for unconfined columns the predicted axial strength, 7.35 MPa, is very closed with the average experimental axial strength, 7.38 MPa.

For strengthened columns, the numerical prediction, of the axial strength, 8.07 MPa, is less than that experimental (average value equal to 9.35 MPa). For all tested specimens, numerical predictions underestimate the experimental results: errors are varying between

5.82% and 27.38%. Those high errors were due to the hypothesis of perfect bond between the steel reinforcement and the matrix. A more reliable analysis has to consider a local bond slip law between the matrix and external reinforcement (in particular, for the steel fibers); however, information about this aspect are very still limited. Actually due to the limited number of experimental results, an analytical form of the local bond-slip law for SRG is not available and its implementation in the numerical procedure is very difficult.

Table 2. Summary of test results [10].

Group	Specimen	Axial stress [MPa]
Control	UC-1	8.72
	UC-2	6.64
	UC-3	6.78
	Abaqus	7.35
Strengthened	C-1-6-0-1	10.28
	C-1-6-0-2	9.46
	C-1-6-0-3	9.14
	C-1-6-0-4	8.54
	Abaqus	8.07

The comparison between numerical predictions and experimental results in terms of axial stress-axial strain curves is described in Figures 4 and 5.

In Fig. 4 the numerical curve is compared with those obtained by tests on un-confined masonry columns. By analyzing the Figure, it appears as the numerical curve provides a good matching of the experimental findings.

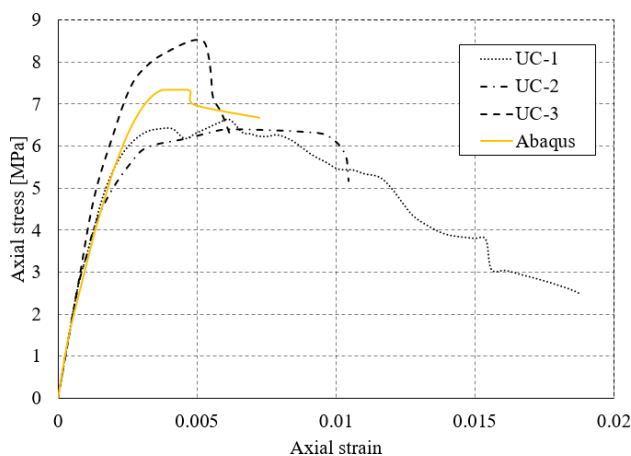


Fig. 4. Experimental-numerical comparison for un-confined columns

The Fig. 5 reports the comparison between the experimental curve corresponding to the confined specimen and the numerical curve.

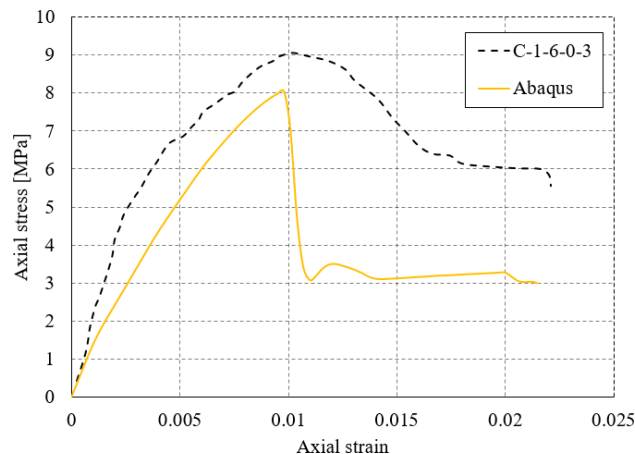


Fig. 5. Experimental and numerical comparison for confined column.

The analysis of the Fig.5 evidences that numerical model furnishes a good prediction in terms of global slip s . Instead, the applied load response is underestimated by the numerical model.

V. CONCLUSION

In the present paper, the contribution of wrapping system made of SRG to masonry columns axial capacity has been investigated. Some experimental results available in the literature are presented and the tests have been simulated with a numerical 3D. The numerical predictions and the experimental results were compared in terms of the peak axial stress and the axial stress-axial strain curves. From this preliminary study emerges that the numerical model furnished good results both in terms of peak stress and in terms of axial stress-axial strain curves. The numerical procedure underestimates the experimental response of confined specimens; this is probably due to the hypothesis of perfect bond between the external steel reinforcement and the matrix assumed in the model. Further improvements of the numerical model can be obtained both considering always a 3D model but where it is possible to set apart the brick and matrix and introducing a local bond-slip law between the steel fibers and the matrix.

REFERENCES

- [1] A. Bruckner, R. Ortlepp, M. Curbach, "Textile reinforced concrete for strengthening in bending and shear", *Mater Struct Rilem*. 2006, 39(6),741-748.
- [2] T.C. Triantafillou, C.G. Papanicolaou, "Shear strengthening of reinforced concrete members with

- textile reinforced mortar (TRM)", *Mater Struct.*, 2006, 39, pp. 93-103.
- [3] C.G. Papanicolaou, T.C. Triantafillou, K. Karlos, M. Papathanasiou, "Textile reinforced mortar (TRM) versus FRP as strengthening material of UMR walls: in plane cyclic loading", *Mater Struct.*, 2007, 40(10), pp. 1081-1097.
- [4] C.G. Papanicolaou, T.C. Triantafillou, K. Karlos, M. Papathanasiou, "Textile reinforced mortar (TRM) versus FRP as strengthening material of UMR walls: out of plane cyclic loading", *Mater Struct.*, 2008, 41(1), pp. 143-157.
- [5] T. Blanksvard, B. Taljsten, A. Carolin, "Shear strengthening of concrete strengthening of concrete structures with the use of mineral-based composites", *J Compos Conctr*, 2009, 13(1), pp. 25-34.
- [6] L. Ombres, S. Verre, "Structural behavior of fabric reinforced cementitious matrix (FRCM) strengthened concrete columns under eccentric load", *Compos Part B*, 2016, 75, pp. 235-249.
- [7] C. Carloni, S. Verre, L.H. Sneed, L. Ombres, "Loading rate effect on the debonding phenomenon in fiber reinforced cementitious matrix-concrete joints", *Compos Part B*, 2017, 108, pp. 301-314.
- [8] T. D'Antino, C. Carloni, L.H. Sneed, C. Pellegrino, "Matrix-fiber bond behavior in PBO FRCM composites: A fracture mechanics approach", *Eng Fract Mech*, 2014, 117, pp. 94-111.
- [9] L.H. Sneed, S. Verre, C. Carloni, L. Ombres, "Flexural behavior of RC beams strengthened with steel-FRCM composite", *Eng Struct*, 2016, 127, pp. 686-699.
- [10] L.H. Sneed, C. Carloni, G. Baietti, G. Fraioli, "Confinement of clay masonry columns with SRG", *Key Eng Mat*, 2017, 747, pp. 350-357.
- [11] Abaqus finite element code, 2011, Hibbitt, Karlsson & Sorensen, Inc, RI.
- [12] F.J. Vecchio, M.P. Collins, "The modified compression-field theory for reinforced concrete elements subjected to shear", *ACI J*, 1986, 83-22, pp. 219-231.
- [13] G.M. Chen, J.G. Teng, J.F. Chen, Q.G. Xiao, "Finite element modeling of debonding failures in FRP-strengthened RC beams: A dynamic approach", *Comput Struct*, 2015, 158, pp. 167-183.
- [14] M. Santandrea, G. Quartarone, C. Carloni, X. Gu, "Confinement of masonry columns with steel and basalt FRCM composites", *Key Eng Mat*, 2017, 747, pp. 342-349.
- [15] Kerakoll S.p.A. –web site: <www.kerakoll.com>; 2017 [accessed Sep 2017].